EFFECT OF CHEMICAL COMPOSITION CHANGE ON MECHANICAL AND MICROSTRUCTURAL PROPERTIES OF ALUMINUM ALLOYS PROCESSED BY SELECTIVE LASER MELTING

[1]Klára NOPOVÁ, [1]Libor PANTĚLEJEV, [2]Daniel KOUTNÝ

[1]Brno University of Technology, Faculty of Mechanical Engineering, Institute of Materials Science and Engineering, Brno, Czech Republic, Klara.Nopova@vutbr.cz, Pantelejev@vutbr.cz

[2]Brno University of Technology, Faculty of Mechanical Engineering, Institute of Machine and Industrial Design Brno, Czech Republic, Daniel.Koutny@vut.cz

https://doi.org/10.37904/metal.2022.4431

Abstract

Additive manufacturing (AM) has been increasingly used to produce metal components in the last few decades. One of the most popular AM technologies is Selective Laser Melting (SLM). Materials prepared by SLM technology show very good mechanical properties, even though in these materials many defects are present, such as spherical pores, keyhole pores, lack of fusion porosity or cracks. The mentioned defects can be minimized by optimizing the process parameters or changing the chemical composition of the material. Therefore, the objective of this study is to describe changes in the microstructure and mechanical properties depending on the Al alloys chemistry. Three new alloys with different chemical compositions (differs in silica content) were prepared by mechanical mixing of the conventional alloys AlSi12 and AlCu2Mg1.5Ni, and subsequently processed by SLM technology with the same process parameters. Relative density (RD), type of defects, and microstructure were studied in all cases by light microscopy (LM). Mechanical properties were determined by tensile tests performed at room temperature and by hardness tests (HV0.3). Fractographic analysis was performed on fracture surfaces after tensile tests using scanning electron microscopy (SEM). It was found that with an increasing percentage of silica, the RD increases from 95.8 % to 98.8 %. The new alloy with the highest Si content showed the highest tensile test characteristics (*UTS* = 453 MPa, *YS* = 243 MPa, and $A_{5.65}$ = 7.74 %). However, the hardness test did not show a significant difference in the values of individual alloys.

Keywords: Selective Laser Melting, aluminum alloys, mechanical properties, microstructure

1. INTRODUCTION

SLM technology allows the production of complex-shaped parts that also have excellent mechanical properties [1]. The mechanical properties are closely related to the microstructural characteristics of the materials. Materials produced by SLM technology have a very fine-grained microstructure due to the rapid solidification of the locally melted material [2,3]. During the process, the laser beam locally melts the material, so that in the final microstructure, the solidified melt pools bounded by fusion boundaries can be observed. The microstructure consists of columnar grains occurring predominantly in the central area of the melt pool and fine equiaxed grains along the fusion boundaries [2,4]. A common problem in materials, especially Al alloys of class 2xxx, produced by SLM technology is the formation of cracks [5]. In general, two types of cracks can be assumed: Liquation and crystallization cracks. Liquation cracks occurred due to the high content of alloying elements. During solidification, the alloying elements, together with impurities, are deposited along the grain boundaries and form liquation films. Crystallization cracks form at the interface between the solid and liquid phases, and their formation is attributed to the high internal stresses resulting from solidification [6]. Studies on the susceptibility to crystallization cracks in Al alloys produced by SLM technology have shown

that crystallization cracks occur more frequently in Al alloys with a low Si content (0.8 wt%) and higher Cu content [2,5,6]. This implies that the occurrence of cracks and pores may be influenced by the process parameters of the SLM technology, but also by the chemical composition of the alloy.

In this study, the influence of Si content on the microstructural and mechanical properties of Al alloys was analysed. AlCu2Mg1.5Ni (EN AW 2618) and AlSi12 were chosen as input materials. The EN AW 2618 offers very good properties and considerable potential for use in the automotive and aerospace industries. Unfortunately, this alloy exhibits many crystallization cracks after the SLM process [5,7]. In contrast, the eutectic AlSi12 alloy is one of the Al alloys with very good processability due to the small temperature difference between liquid and solid [5]. Increasing the Si content (and decreasing the Cu content) seems to be very promising, and that was the motivation for this study.

2. INPUT MATERIALS

AlCu2Mg1.5Ni (EN AW 2618) in powder form was chosen as the input material. The chemical composition was determined by ICP-OES spectrometer (Therm iCAP 6500-ICP) (**Table 1**). The change of chemical composition of EN AW 2618 by willful increase of Si (decrease of Cu) was done by mixing this alloy with AlSi12 alloy in powder form. The AlSi12 alloy was prepared by atomization in an inert gas; the chemical composition [8] can be found in **Table 1**. These two powders were mechanically mixed for 24 hours using a TWINROLL mixer. Three new mixtures were prepared: Mixture “I” 75 wt% AlSi12 + 25 wt% EN AW 2618, the mixture “II” 50 wt% AlSi12 + 50 wt% EN AW 2618 and the last mixture “III” 25 wt% AlSi12 + 75 wt% EN AW 2618, the chemical composition of the new blends is listed in **Table 1**.

Table 1 Chemical composition of input material (wt%)

	Si	Fe	Cu	Mg	Ni	Al
EN AW 2618	0.15	1.00	2.66	1.39	1.22	Balance
Mixture I	9.04	0.85	0.89	0.42	0.30	Balance
Mixture II	6.08	0.90	1.48	0.75	0.61	Balance
Mixture III	3.10	0.95	2.07	1.06	0.91	Balance
AlSi12 [8]	11.80	0.13	<0.01	<0.01	<0.01	Balance

3. EXPERIMENTAL METHODS

Four bulk specimens with dimensions of 12×12×70 mm were produced from each individual powder mixture by the SLM 280 HL (SLM Solution GmbH). The machine was equipped with a 400 W YLR fiber laser with 3D scanning optics and a build chamber of 280×280×350 mm.

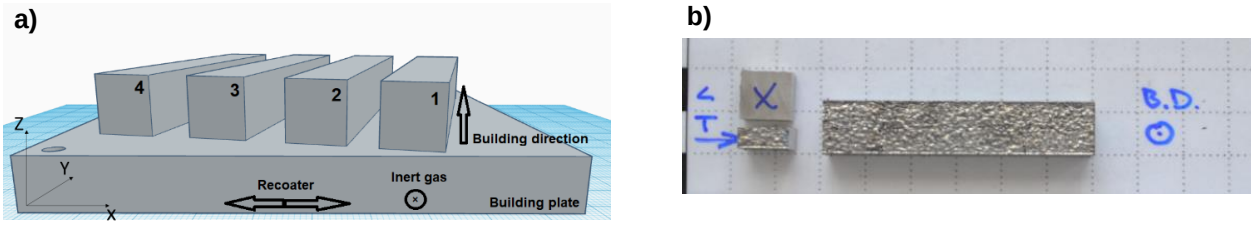

Figure 1 a) Bulk specimens on the build platform, b) analysed planes (B.D. – building direction)

The process parameters used are the following: laser power 400 W, scanning speed 1200 mm/s, hatch distance 0.09 mm, layer thickness 0.05 mm, scanning strategy Stripe, rotation between layers 67° and nitrogen as inert gas. The specimens were printed horizontally, as shown in **Figure 1a**.

All specimens were analysed in the as-built condition. Tensile specimens were machined from billets No. 1–3 for each new alloy according to DIN 50125 (Form B, gauge length of ø6×30 mm). Tensile testing at room temperature was performed using the Zwick Z250 testing machine equipped by the extensometer MultiXtens with a loading rate of 2 mm/min. Fractographic analyses were performed for all broken specimens after the tensile test using SEM (Zeiss Ultra Plus). Billet No. 4 (for each alloy) was used for the microstructural analysis in two directions: transverse – T (plane YZ) and longitudinal – L (plane XZ), shown **Figure 1b**. The microstructures were examined by light microscopy (LM) in the non-etched and etched states (etchant: 0.7 vol%, HF; 2.4 vol% HCl; 0.8 vol% HNO_3; 96.1 vol% distilled water). The relative density (RD) was determinate in non-etched state for both directions (L and T) using ImageJ software. Vickers hardness tests was performed using the Q-ness hardness tester (Q10A) with a load of 0.3 kg (HV0.3) for 10 s.

4. RESULTS

4.1. Microstructural analysis

The analyses confirmed the assumed influence of the chemical composition on RD of the material, **Figure 2**. Alloy “I” shows irregularly distributed spherical gas pores in the material volume (RD = 98.8 %). The lack of fusion porosity was observed in the second case alloy “II”, which had RD = 96.8 %. The last alloy “III” exhibited many cracks that follow the building direction (RD = 95.8 %).

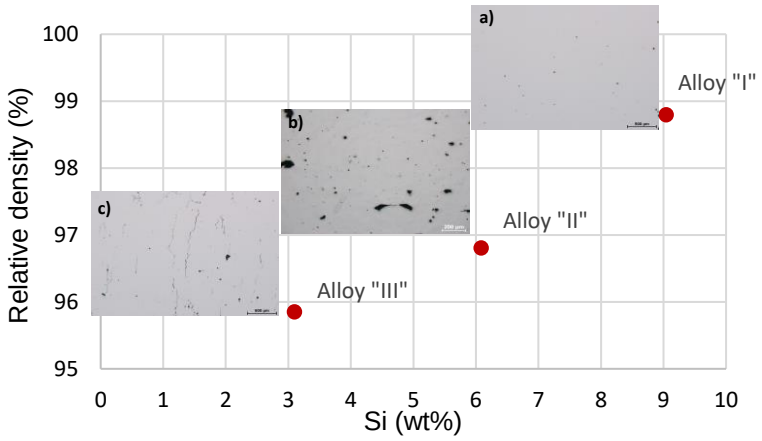

Figure 2 The dependence of RD on Si content: a) alloy “I” – gas pores; b) alloy “II” – lack of fusion porosity; c) alloy “III” – cracks

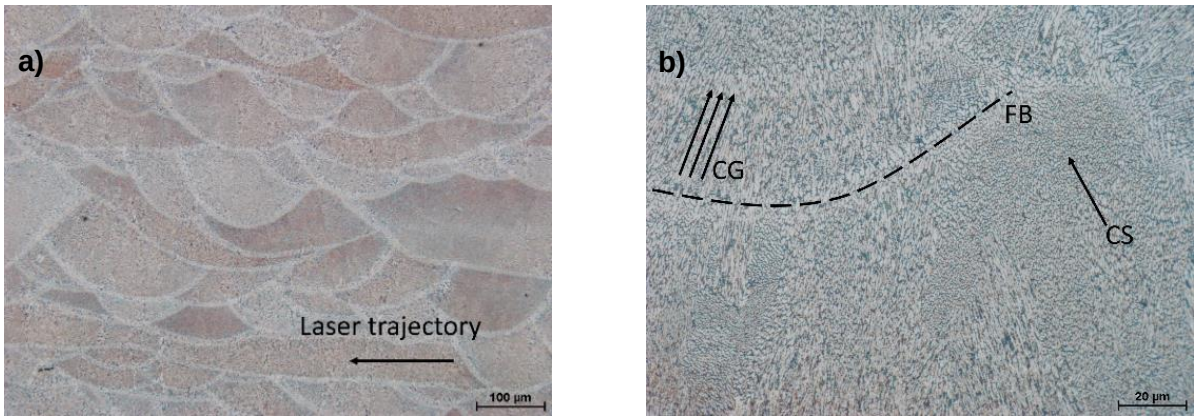

Figure 3 Microstructure of Alloy “I” in longitudinal direction: a) melting pools; b) columnar grains (CG), cell microstructure (CS) and fusion boundaries (FB); LM

Figure 3 shows the microstructure of alloy "I" after the SLM process, while alloys "II" and "III" have a similar microstructure. Both investigated directions L and T exhibited the typical fish-scale shape of melt pools bordered by fusion boundaries (FB). In addition, using lower magnification, a laser trajectory is observed in some layers, caused by the rotation of the laser scanning strategy between layers. In a detailed analysis, the appearance of a very fine cell microstructure (CS) and the presence of columnar grains (CG) can be observed in some melt pools.

4.2. Mechanical properties and fractographic analysis

Table 2 shows the average mechanical values for each of the new alloys as well as the conventional alloys. The *UTS* of the alloy "III" is comparable to that of the alloy EN AW 2618. *YS* could not be measured for this alloy due to premature fracture. The highest value of *YS* (277 MPa) was for the alloy "II" despite the frequent occurrence of defects in the material. Alloy "I" had the highest *UTS* (453 MPa) and $A_{5.65}$ (7.7%), which may be due to the highest values of RD. The hardness test showed very similar results for all new alloys as follow: alloy "I" 124 ± 4 HV0.3; alloy "II" 133 ± 1 HV0.3 and alloy "III" 132 ± 3 HV0.3.

Table 2 Average values of tensile tests at room temperature [7, 9]

	***UTS* (MPa)**	***YS* (MPa)**	**$A_{5.65}$ (%)**
AlSi12	385	260	2.8
Alloy I	453	243	7.7
Alloy II	400	277	3.5
Alloy III	192	-	0.1
EN AW 2618	191	177	0.6

Figure 4 shows the fracture surface of the specimens of the new alloys processed by SLM. The fracture surface of the specimens shows areas with decohesion along columnar grains and areas with very fine dimple morphology (**Figure 4a**), indicating the low-energetic ductile fracture. The alloy "II" shows areas with lack of fusion porosity (pores with unmelted powder particles). The decohesion along the columnar grains was observed on the fracture surfaces of each alloy, especially for the alloy "III" (**Figure 4b**).

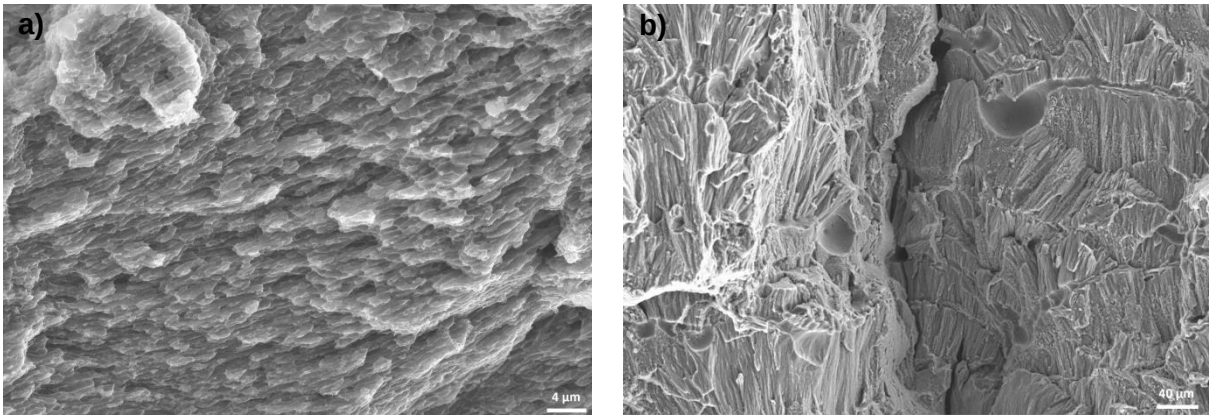

Figure 4 SEM – fracture surface: a) alloy "I" – dimple morphology; b) alloy "III" – decohesion along columnar grains and pores

5. DISCCUSION

The microstructure of the alloys studied showed a typical occurrence of fish-scale shape structure resulting from uniformly shaped melt pools during the process, as well as visible laser trajectories [10]. In all three new

alloys studied, the size of the melt pools was comparable, which can be attributed to the same process parameters. The presence of columnar grains in the melt pools was detected, and a very fine cell microstructure was observed as in the study [10]. The highest relative density was obtained for alloy "I" (98.8 %), this alloy showed predominantly spherical pores, moreover solidification cracks were eliminated, due to the higher Si content. Similar results showed the study [11] where the authors have used alloy Al7075 and confirmed that only 2 wt% of Si significantly affects the occurrence of cracks and pores in the microstructure. The alloy "III" showed the worst relative density (95.8 %), for this alloy the occurrence of large solidifications cracks was noted. The difference in the behavior of the alloys can be attributed to a different chemical composition.

The tensile tests showed the increase of *UTS* and $A_{5.65}$ with increasing RD. Alloy "I" showed the highest elongation at break ($A_{5.65}$ = 7.7%), which is due to the highest RD of the specimens and absence of solidification cracks. The highest *YS* value had the alloy "II" although the lack of fusion porosity was observed on the fracture surface. The alloy "III" showed almost no elongation, mainly due to the extensive cracks in the material. The UTS value of the alloy "III" is comparable with the input alloy EN AW 2618 due to the appearance of numerous cracks that reduced the load-bearing cross section of the specimens. The results show that the alloys "I" and "II" have better properties after SLM process that the conventional input alloys and better than the alloy AlSi10Mg as well [7, 12, 13]. Comparing the hardness of the new alloys HV0.3 (~130 HV0.3) with the conventional alloy EN AW 2618 (~100 HV0.3) [7], all new alloys show higher hardness values.

Fractographic analysis showed a low energetic ductile fracture with very fine dimple morphology. Inhomogeneities such as lack of fusion porosity and spherical pores were observed on the fracture surface of all alloys, and decohesion along the columnar grains and fusion boundaries was observed as well. The lowest percentage of defects was observed for the alloy with the highest Si content. This is in contrast to [7], where a significant lack of fusion porosity level was observed in the alloy EN AW 2618, which was processed by the SLM technology. It can therefore be assumed that not only the Si content, but also the Cu content has a significant influence on the resulting microstructure of Al alloys produced by SLM technology [14].

6. CONCLUSIONS

- Three new alloys were produced by mixing of conventional alloys AlSi12 and EN AW 2618. The new alloys were processed by SLM technology with the same process parameters.
- Metallographic and fractographic analyses showed that cracks and pores in the microstructure of the material are suppressed with increasing Si content (decreasing Cu content).
- The mechanical properties, especially UTS, significantly affected the number of pores and cracks in the microstructure. Samples with a higher percentage of cracks and inhomogeneities of the void type showed the lowest values of mechanical properties. The hardness values were comparable for all alloys studied.
- Fractographic analysis showed a low-energetic ductile fracture with fine dimple morphology.

ACKNOWLEDGEMENTS

Authors acknowledge the financial support received from the projects FSI-S-20-6290 and CZ.02.1.01/0.0/0.0/16_025/0007304.

REFERENCES

[1] TRODELLO, A., FIOCHI, J., BIFFI, C.A., CHIANDSSI, G., ROSSETTO, M., TUISSI, A., PAOLINO, D. S. VHCF response of Gaussian SLM AlSi10Mg specimens. Effect of a stress relief heat treatment. *International Journal of Fatigue*. 2018, vol. 124, pp. 435-443.

[2] OLAKANMI, E.O., COCHRANE, R.F., DALGARNO, K.W.A. A review on selective laser sintering/melting (SLS/SLM) of aluminium alloy powders: Processing, microstructure, and properties. *Progress in Materials Science.* 2015, vol. 74, pp. 401– 477.

[3] HERZOG, D., SEYDA, V., WYCISK, E. Additive manufacturing of metals. *Acta Materialia.* 2016, vol. 117, pp. 371-392.

[4] THIJS, L., KEMPER, K., KRUTH J.P., VAN HUMBEECK, J. Fine-structure aluminium products with controllable texture by selective laser melting of pre-alloyed AlSi10Mg powder. *Acta Materialia*. 2013, pp. 1809-1819.

[5] GALY, C., LE GUEN, E., LACOSTE, E., ARVIEU, C. Main defects observed in aluminum alloy parts produced by SLM: From causes to consequences. *Additive Manufacturing*. 2018, vol. 22, pp. 165–175.

[6] CAO, X., WALLACE, W., IMMARIGEON, J.P. Research and progress in laser welding of wrought aluminum alloys. II. Metallurgical microstructures, defects, and mechanical properties. *Materials and Manufacturing Processes*. 2003, vol. 18, pp. 23-49.

[7] KOUTNÝ, D., PALOUŠEK, D., PANTĚLEJEV, L., HOELLER, CH., PICHLER, R. Influence of scanning strategies on processing of aluminum alloy EN AW 2618 using Selective Laser Melting. *Materials*. 2018, vol. 11, pp. 2 - 18.

[8] EN 18273, *European Steel and Alloy Grades*, Kharkov, Ukraine, 2011.

[9] PRASHNATH, K.G., SCUDINO, S., ECKERT, J. Defining tensile properties of Al-Si12 parts produced by selective laser melting. *Acta materialia*. 2017, pp. 25-35.

[10] LI, L., LI, R., YUAN, T., CHEN, C., ZHANG, Z., LI, X. Microstructures and tensile properties of a selective laser melted Al–Zn–Mg–Cu (Al7075) alloy by Si and Zr microalloying. *Materials Science and Engineering: A.* February 2020, vol. *787*, p. 139492.

[11] MONTERO-SISTIAGA, M.L., MERMETNS, R., VRANCKEN, B., WANG, X., HOOREWEBER B.V., KRUTH J-P., HUMBEECK, J. Changing the alloy composition of Al7075 for better processability by selective laser melting. *Journal of Materials Processing Technology*. 2016, pp. 437-445.

[12] PRASHNATH, K.G., SCUDINO S., ECKERT, J. Defining tensile properties of Al-12Si parts produced by selective laser melting. *Acta Materialia*. 2017, pp. 25-35.

[13] TIWARI, J.K., MANDAL, A., SATHISH, N., AGRAWAL, A.K., SRIVASTAVA, A.K. Investigation of porosity, microstructure and mechanical properties of additively manufactured graphene reinforced AlSi10Mg composite. *Additive Manufacturing*. 2020, vol. 33, p. 101095.

[14] BAITIMEROV, R., LYKOV P., ZHEREBTSOV, D. Influence of powder characteristics on processability of AlSi12 alloy fabricated by selective laser melting. *Materials*. 2018, vol. 11, p. 742.